ELSEVIER

1 January 1998

OPTICS COMMUNICATIONS

Optics Communications 145 (1998) 291–299

Full length article

Spectral shifts and line-shapes asymmetries in the resonant response of grating waveguide structures

S. Glasberg *, A. Sharon, D. Rosenblatt, A.A. Friesem

Department of Physics of Complex Systems, Weizmann Institute of Science, Rehovot 76100, Israel

Received 13 May 1997; accepted 28 July 1997

Abstract

The resonant spectral response that grating-waveguide structures display in the transmitted and reflected intensities, is analyzed with the aid of a newly developed wave interference model. The resonant response is shown to be generally accompanied by wavelength shifts for the transmitted and reflected intensities, resulting in asymmetric resonance line-shapes. A simple rule that relates the ratio of these resonant shifts to the reflected intensity from the structure away from resonance is obtained. The predicted results from the model were confirmed experimentally with both dielectric as well as metal based grating-waveguide structures. © 1998 Elsevier Science B.V.

PACS: 42.79.Gj; 73.20.Mf
Keywords: Resonance; Line-shape; Grating-waveguide structures; Surface-plasmon

1. Introduction

Diffraction properties of multilayer dielectric and metal based grating-waveguide structures (GWS), comprised of a substrate, a thin waveguide layer, and a grating, have been investigated for some time. These structures display a resonant response to an incident plane wave, which is due to a coupling process between the incidence wave and a guided mode within the structure. The investigations originated in studies on diffraction anomalies, from metallic gratings, that were first observed by Wood [1] in 1902 for TM polarization and partially explained by Rayleigh in 1907 [2]. Fano [3] suggested that the diffraction anomalies occur due to some resonant coupling process. He accounted for a surface EM resonance which was subsequently noted by Ritchie [4] as the surface plasmon. Later, Hessel and Oliner presented a phenomenological model [5] in which such anomalies could be attributed to the excitation of surface waves of which surface plasmons are only one class. They showed that in the immediate vicinity of the resonance, the reflection anomaly could be generally represented by a simple pole-zero function in the complex wave-vector. Neviere [6] generalized this picture to include waveguides.

Recently, the investigations were directed to determine the influence of the resonant coupling on the intensities of the reflected and transmitted zero order diffracted waves [7–16]. Specifically, transparent dielectric and semiconductor GWS were found to strongly reflect the incident plane wave, within a narrow bandwidth in which the resonant coupling occurs [7–14]. Also, reflective metal based GWS (MB GWS) were shown to display a strong absorption of the incident plane wave within a narrow bandwidth [15,16].

In general, the response of grating waveguide structures is not entirely a symmetric Lorentzian one, but also includes substantial side-lobes. Under certain conditions, the resonant line-shapes even become completely asymmetric [14]. Some numerical studies clearly indicated that the appearance of side-lobes is due to Fresnel reflections from

* Present address: Department of Condensed Matter Physics, Weizmann Institute of Science, Rehovot 76100, Israel. E-mail: hshmil@wis.weizmann.ac.il.

PII S0030-4018(97)00447-1

interfaces [17,18], which modify the response at resonance. An anti-reflection waveguide geometry was suggested [17] for reducing the side-lobes in semi-transparent dielectric structures. Indeed, in some cases, highly symmetric response can be obtained with common anti-reflection coatings [13]. Nevertheless, the asymmetric resonance lineshapes are still present in many dielectric and semi-conductor structures as well as in metallic structures used for surface plasmon studies [19].

In this paper, we exploit an analytic interference [16] model to determine the dependence of the resonance response, in both dielectric and metal based GWS, on the structures geometrical and optical parameters. Specifically, we show that the asymmetries in the transmitted and reflected intensities are due to spectral shifts and that these shifts originate from radiative coupling terms. A simple rule that relates the ratio of these resonant shifts to the reflected intensity away from resonance, provides quantitative results. These results reduce to a simple symmetric resonance behaviour at the limits of either completely transparent or fully reflective grating waveguide structures.

In the following, we characterize dielectric and metal based GWS, and describe the modes they support. Then, we utilize the interference model to investigate the resonant response, and especially the wavelength shifts. We also analyze the resonant response with a rigorous numeri-

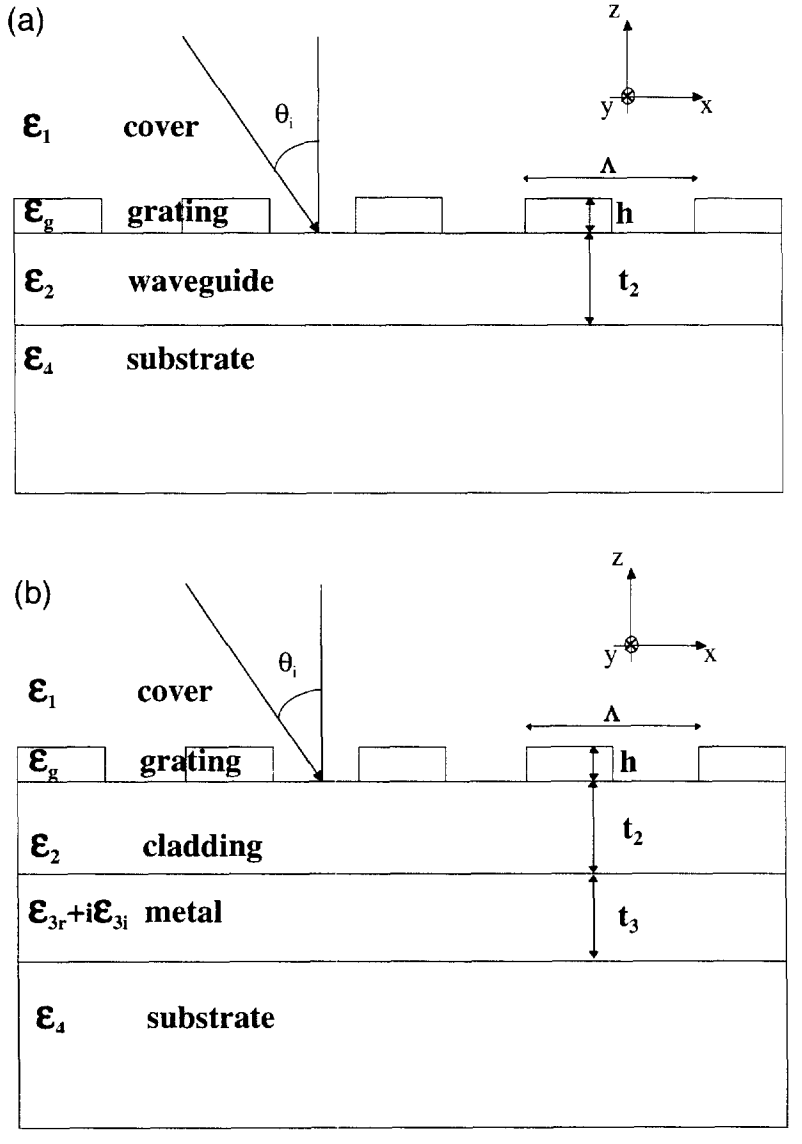

Fig. 1. Geometry of grating-waveguide structures (GWS): (a) dielectric; (b) metal based.

cal model and compare the results with those from the interference model. Finally, we present experimental results with dielectric GWS as well as metal based GWS.

2. Basic structures and propagating modes

The basic dielectric and metal based GWS are shown in Fig. 1. The dielectric GWS, shown in Fig. 1a, is comprised of a relief grating, a waveguide layer and a substrate. The MB GWS, shown in Fig. 1b, has an additional metal layer and the waveguide layer serves as a cladding layer. The grating periodicity is denoted by Λ, its depth by h, and its dielectric constant by ϵ_g. Between and above the grating grooves the dielectric constant is denoted by ϵ_1, which typically is 1. The waveguide (cladding) layer thickness is denoted by t_2, and its dielectric constant by ϵ_2. The metallic layer thickness is denoted by t_3, and its complex dielectric constant is ϵ_3, where $\epsilon_3 = \epsilon_{3r} + i\epsilon_{3i}$. The substrate thickness is assumed to be infinite, where its dielectric constant is ϵ_4. The structures are illuminated with an incident plane wave at an angle θ_i. Only a single interface in either structure is assumed to reflect the incident plane wave. In metal based GWS, it is the metal layer while in dielectric GWS it is one of the substrate facets. All other interfaces are assumed to be transparent for any incident wave. This assumption is valid for structures made of dielectric materials having similar refractive indexes, and anti-reflection coated to avoid multiple reflections. As an approximate model it can be used when additional reflections are weak enough to result in a minor modification of the prime reflected amplitude. Two orthogonal polarizations are possible for the incident wave: The TM polarization where the magnetic vector of the wave is parallel to the grating grooves (i.e., parallel to y-axis), and the TE polarization where the electric field vector of the wave is parallel to the grating grooves.

In order to describe the various modes that propagate in a GWS, we begin with a simplified structure in which there is no grating. For the dielectric GWS, the relevant multi-layer model is the three slab dielectric waveguide (substrate–waveguide–air) that supports either TM or TE modes [20]. For the MB GWS, the guiding layer can be either the metal layer or the cladding layer. When this metal layer is thick (usually more than 100 nm), two de-coupled surface plasmons exist as the fundamental TM modes, one for the upper and one for the lower metal–dielectric boundaries. The structure with the thick metal layer supports, either in TE or TM polarizations, bound dielectric modes that propagate in the cladding [15,16,19]. As the thickness of the metal layer decreases, the two surface plasmon modes become coupled and turn into long-range and short-range plasmon modes. In a structure with symmetric configuration, that is, when the two metal–dielectric boundaries are identical, it was found that as the thickness of the metal layer tends to zero, the dissipative loss of the long-range surface plasmon tends to zero [21]. The role of the cladding layer is to approach a symmetric configuration, in order to lower the cutoff thickness of the metal layer for the existence of the coupled plasmon modes [22]. A MB GWS which is designed to support the long range and short range surface plasmons does not support, in TM polarization, higher order bound dielectric modes. However, it does support the TE_0 mode, that radiates energy into the substrate as it propagates, hence this is a highly lossy mode. We note that the loss, for dielectric GWS, is always attributed to undesirable scattering due to structure imperfections, which degrades the resonance behaviour. For MB GWS, the loss is attributed to absorption of the propagating mode, and is essential for having resonant behaviour.

We now proceed to the complete structure in which a thin grating is added to the simplified structure. At and near resonance, the grating can couple light into and out of the waveguide by diffraction. The addition of the grating can be considered as a small perturbation to the waveguide which results in slight changes in the envelope and propagation constant of the propagating mode. The height of the grating is typically much smaller than the illuminating wavelength λ_0. The grating period is of the order of λ_0/n_2, where $n_2 = \sqrt{\epsilon_2}$, so the first diffracted orders into the structure are propagating, whereas the higher diffraction orders are evanescent. The first order diffraction occurs in accordance to: $2\pi/\Lambda = \pm n_1 k_0 \sin\theta_i + \beta_r$, where Λ is the grating period, $k_0 = 2\pi/\lambda_0$, θ_i is the incident angle of the incoming wave, and β_r is the real part of the mode propagation constant, $\beta = \beta_r + i\beta_i$.

3. The analytic model

In order to analyze the resonance response of GWS, it is convenient to exploit an analytic interference model [16], that was originally applied to a limiting (and degenerate) case of fully reflective metal based GWS. Here, the model is adopted to analyze GWS with arbitrary reflectivities away from resonance. Accordingly, the analytic expressions for the resonant response of the reflected and transmitted field amplitudes are given by

$$r(\Delta) = e^{i\phi}\frac{-(r_0\Delta + S\sin\phi) + i(S(r_0 - \cos\phi) - \alpha r_0)}{(\Delta + Sr_0\sin\phi) + i(S(1 - r_0\cos\phi) + \alpha)},$$

$$t(\Delta) = t_0\frac{\Delta + i\alpha}{(\Delta + Sr_0\sin\phi) + i(S(1 - r_0\cos\phi) + \alpha)}. \quad (1)$$

The corresponding expressions for the normalized reflected and transmitted intensities are

$$R(\Delta)=\frac{(r_0\Delta+S\sin\phi)^2+(S(r_0-\cos\phi)-\alpha r_0)^2}{(\Delta+Sr_0\sin\phi)^2+(S(1-r_0\cos\phi)+\alpha)^2},$$

$$T(\Delta)=t_0^2\frac{\Delta^2+\alpha^2}{(\Delta+Sr_0\sin\phi)^2+(S(1-r_0\cos\phi)+\alpha)^2}. \tag{2}$$

In Eqs. (1) and (2), r and t, and R and T are the reflected and transmitted amplitudes and intensities respectively, r_0^2 and t_0^2 are the reflected and transmitted intensities away from resonance, $r_0^2+t_0^2=1$, S is the grating diffraction parameter, ϕ is the total phase difference due to optical path in the cladding and the Fresnel phase at reflection, α is the mode loss, and Δ is the dephasing from resonance condition, where S, Δ, α are dimensionless. For a thin grating of height h, $S\propto(\Delta\epsilon\xi_{\pm1}\Lambda h/\lambda^2)^2$, where $\Delta\epsilon$ is the dielectric constant modulation in the grating region, namely $\Delta\epsilon=\epsilon_g-\epsilon_1$, and $\xi_{\pm1}$ are the first Fourier components of the grating. The mode loss, α, equals β_i/k_0. Eqs. (1) were obtained using the approximations S, Δ, $\alpha\ll1$, i.e., we assumed thin grating, spectral response near resonance and small mode loss. Note, Eqs. (2) reduce to simple Lorentzian forms, in the limiting cases of either completely transparent ($r_0\to0$) or fully reflective structures ($r_0\to1$), to yield

$$R(\Delta)=\frac{S^2}{\Delta^2+(S+\alpha)^2},\quad T(\Delta)=\frac{\Delta^2+\alpha^2}{\Delta^2+(S+\alpha)^2},$$

for $r_0\to0$,

$$R(\tilde{\Delta})=\frac{\tilde{\Delta}^2+(\tilde{S}-\alpha)^2}{\tilde{\Delta}^2+(\tilde{S}+\alpha)^2},\quad T(\tilde{\Delta})=0,\quad \text{for } r_0\to1, \tag{3}$$

where $\tilde{\Delta}=\Delta+S\sin\phi$ and $\tilde{S}=S(1-\cos\phi)$.

Away from resonance ($\Delta\gg S$, α), Eq. (3) reduce to the expected smooth spectral response of a coated metallic mirror (in MB GWS), or of a transparent structure (in dielectric or semiconductor GWS). At resonance (Δ, $\tilde{\Delta}=0$), sharp change in the reflected and transmitted intensities can occur; for the transparent GWS the reflected intensity can reach one, if $S\gg\alpha$; for the fully reflective MB GWS the reflected intensity can drop to zero, if $\tilde{S}=\alpha$.

Using Eq. (2), we calculated the resonance behaviour for specific dielectric and metal based GWS. The results for the normalized reflected and transmitted intensities and loss as a function of the dephasing from mode condition, Δ/S, are shown in Figs. 2 and 3; the parameters for the GWS are given. As it is evident, the response has not symmetric Lorentzian behaviour. At resonance, we can see a rise in the reflected intensity in the dielectric structure (Fig. 2) versus a fall in the reflected intensity from the metal based structure (Fig. 3).

In order to understand the origin of the asymmetries in the lineshapes shown in Figs. 2 and 3, we first perform the transformation $\tilde{\Delta}=\Delta-Sr_0\sin\phi$ in Eq. (1), in order to account for mode displacement due to coupling with the incident wave. Then, we decompose each of the resulting equations for the intensities into a quadratic and non-quadratic terms, to yield

$$R(\tilde{\Delta})=\frac{r_0^2\tilde{\Delta}^2+(t_0^2S\sin\phi)^2+(S(r_0-\cos\phi)-\alpha r_0)^2}{\tilde{\Delta}^2+(S(1-r_0\cos\phi)+\alpha)^2}+2r_0t_0^2S\sin\phi\frac{\tilde{\Delta}}{\tilde{\Delta}^2+(S(1-r_0\cos\phi)+\alpha)^2},$$

$$T(\tilde{\Delta})=t_0^2\frac{\tilde{\Delta}^2+(Sr_0\sin\phi)^2+\alpha^2}{\tilde{\Delta}^2+(S(1-r_0\cos\phi)+\alpha)^2}-2r_0t_0^2S\sin\phi\frac{\tilde{\Delta}}{\tilde{\Delta}^2+(S(1-r_0\cos\phi)+\alpha)^2}. \tag{4}$$

The quadratic term in each equation has a Lorentzian symmetric form. The non-quadratic terms are identical, but with opposite sign. The coupling process of the reflected amplitude r_0 to the waveguide, as represented by the term $Sr_0\sin\phi$, leads to monotonic displacement of the resonance spectral location and interference. The displacement was accounted for by the transformation $\tilde{\Delta}=\Delta-Sr_0\sin\phi$. The interference occurs in the waveguide between one mode amplitude and another that is delayed by the phase shift ϕ, and produces the non-quadratic intensity variations. In the limits of either completely transparent or fully reflective GWS, the non-quadratic term vanishes. Hence, at both of those limits we can expect the observed Lorentzian responses [13,16].

On the other hand, the loss (or absorption), that occurs when a mode is excited, always has a Lorentzian form. This could be predicted from Eq. (4), where the loss is calculated as $1-(R+T)$, and shown in Figs. 2 and 3. Assuming that the loss is maximal for the wavelength at which the dephasing from mode condition is zero, we identify the wavelength at which the peak loss occurs as the resonant wavelength. Similarly, we can characterize the resonance behaviour of the reflected and transmitted intensities by the spectral location of their minima. Specifically, the reflection and transmission minima in Figs. 2 and 3 are spectrally shifted with respect to the peak loss. We denote those spectral shifts as $\Delta\lambda_r$ and $\Delta\lambda_t$. A convenient and general rule for the ratio of these shifts can be obtained from Eq. (2).

The numerator and the denominator in the expression for R (as well as for T) in Eq. (2) are minimal at different

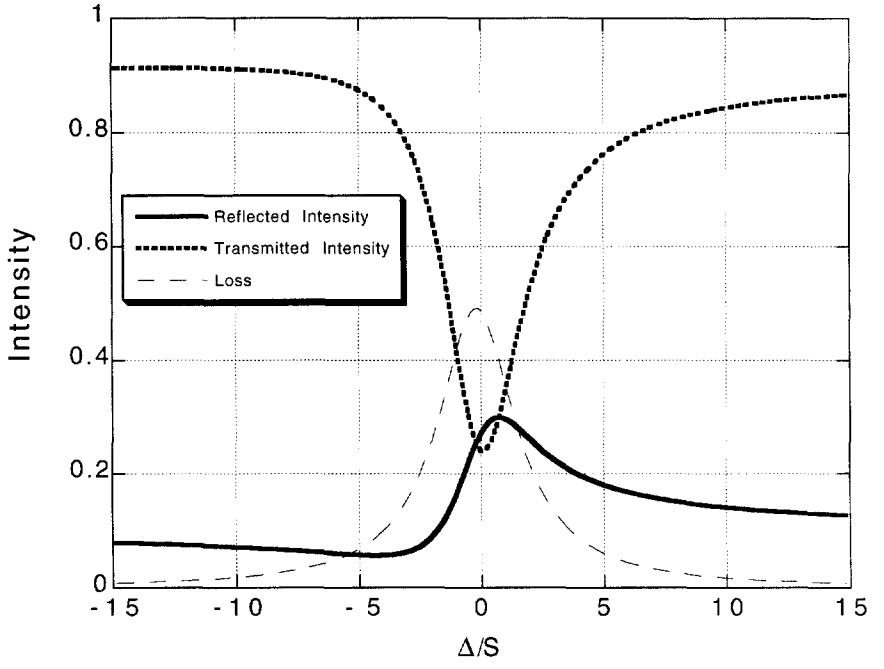

Fig. 2. Analytic calculation for the reflected and transmitted intensities and the loss as a function of the dephasing ratio, Δ/S, for dielectric GWS. $r_0^2 = 0.1$, $t_0^2 = 0.9$, $\alpha/S = 1$, and $\sin\phi = 0.62$.

values of Δ. We denote these differences for R as Δ_r and for T as Δ_t, where $\Delta_r = Sr_0\sin\phi - (S/r_0)\sin\phi$ and $\Delta_t = Sr_0\sin\phi$. Simple calculation yields: $\Delta_r/\Delta_t = -t_0^2/r_0^2$. For the special case of $\Delta\lambda_r/\lambda_0 = \Delta_r$ and $\Delta\lambda_t/\lambda_0 = \Delta_t$, which occurs only when both broadening mechanisms of loss α and radiative coupling $S(r_0 - \cos\phi)$ equal to

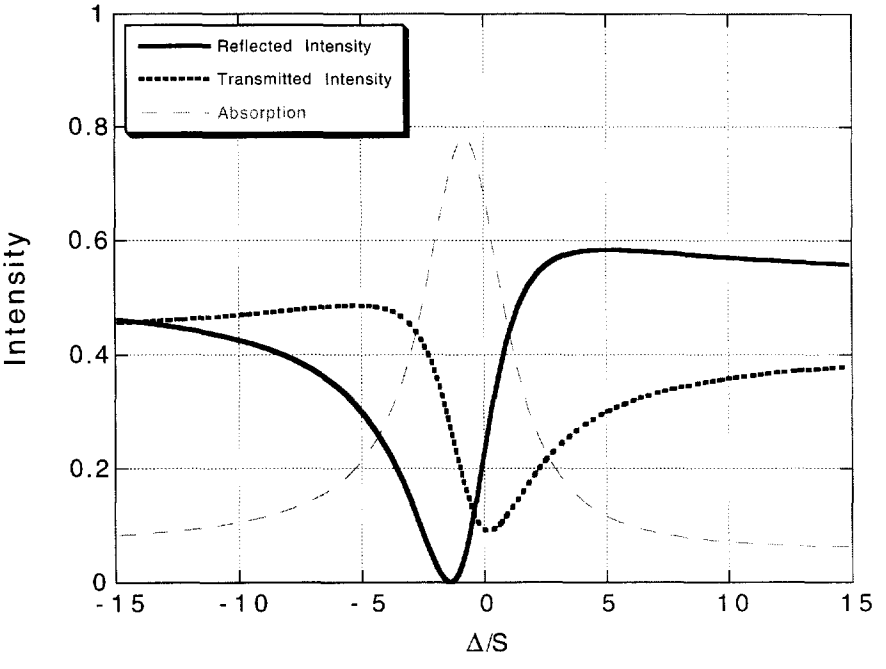

Fig. 3. Analytic calculation for the reflected and transmitted intensities and the absorption as a function of the dephasing ratio, Δ/S, for MB GWS. $r_0^2 = 0.52$, $t_0^2 = 0.41$, $\alpha/S = 1$, and $\sin\phi = 1$.

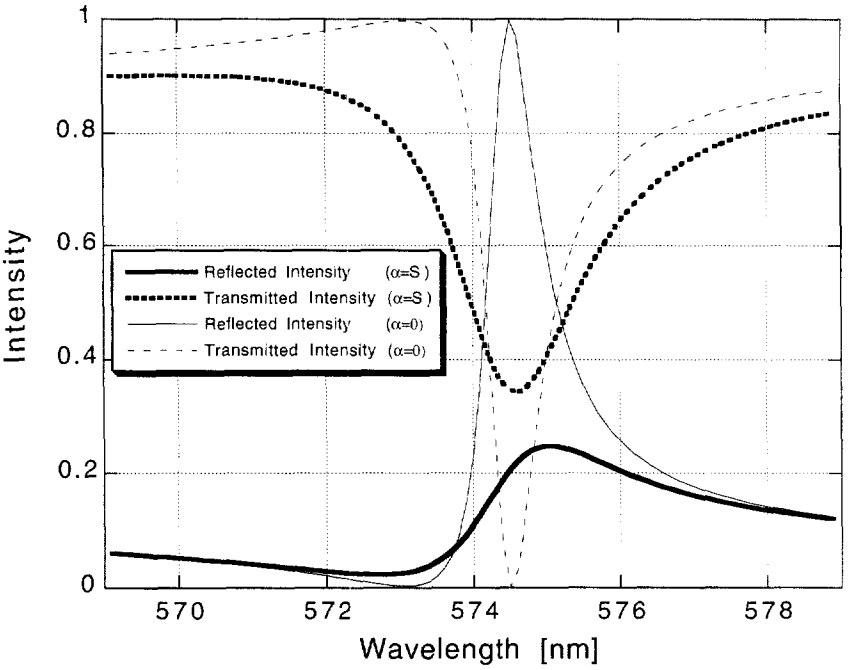

Fig. 4. Numerical calculation for the reflected and transmitted intensities as a function of wavelength for the dielectric GWS, with and without presence of losses.

zero, $\Delta\lambda_r/\Delta\lambda_t = -t_0^2/r_0^2$. In general, $\Delta\lambda_r/\lambda_0 > \Delta_r$ and $\Delta\lambda_t/\lambda_0 > \Delta_t$. The increase shifts occur simultaneously, so the following generally holds:

$$\Delta\lambda_r/\Delta\lambda_t \approx -t_0^2/r_0^2. \tag{5}$$

Eq. (5) indicates that the ratio of the wavelength shifts in the reflection and transmission minima with respect to the resonant wavelength is about inversely proportional to the ratio of the reflected to transmitted intensities, away from resonance. This ratio provides a quantitative criteria as to how much a given structure deviates from the symmetric response that characterizes either fully transparent structures (where this ratio gives infinity) or fully reflective structures (where the ratio equals zero). Substituting values in Eq. (5), taken from Figs. 2 and 3, we obtain for the dielectric GWS, $\Delta\lambda_r/\Delta\lambda_t \cong -8$ versus $t_0^2/r_0^2 = 9$, and for the MB GWS, $\Delta\lambda_r/\Delta\lambda_t \cong -3/4$ versus $t_0^2/r_0^2 \cong 4/5$. Finally, we note that the shift between the minimum of transmission and the peak of reflection for the dielectric GWS is not due to a spectral shift. Rather, it is the effect of the loss α (see Fig. 4). For this nearly transparent structure, the minimum of the reflected intensity occurs at $\Delta/S = -4$, and is less pronounced.

4. The numerical model

In order to determine the exact electromagnetic field distribution in the GWS, we exploited a numerical model, which is based on Maxwell's equations, and the exact eigen-function approach [23]. From this model we found the exact solution for the spectral response of dielectric and metal based GWS.

A representative result of our calculations for a dielectric GWS, which supports the TE_0 mode, is presented in Fig. 4. This result was obtained for a structure having a grating with a period of 290 nm, a height of 60 nm, duty cycle half and a dielectric constant of 4.2, a waveguide layer with thickness of 410 nm and a dielectric constant of 4.2, and a substrate with dielectric constant of 2.28. Fig. 4 shows the normalized reflected and transmitted intensities, at and near resonance, as a function of wavelength, when the angle of the incident plane wave is oriented at zero degrees with respect to the normal. The responses are for lossless structure where $\alpha = 0$ and for a lossy structure with $\alpha \cong S$. The ratio of the spectral shifts with respect to the resonant wavelength at 574.4 nm, for $\alpha = S$, is $\Delta\lambda_r/\Delta\lambda_t \cong -8.5$, versus $t_0^2/r_0^2 \cong 9$. In addition, only when $\alpha \cong S$, we note a shift, of about 0.4 nm, between the peak in reflection and the minimum of transmission. As the loss α increases, the variation in intensities from resonance to non-resonance decreases and the spectral bandwidths at FWHM broaden. As it is evident, the spectral bandwidth of the transmitted intensity at FWHM increases from about 1 nm for a structure with no loss to about 2 nm for a structure with loss.

The result of our calculations for a MB GWS, which supports the long-range surface plasmon, is presented in Fig. 5. This result was obtained for a structure having a

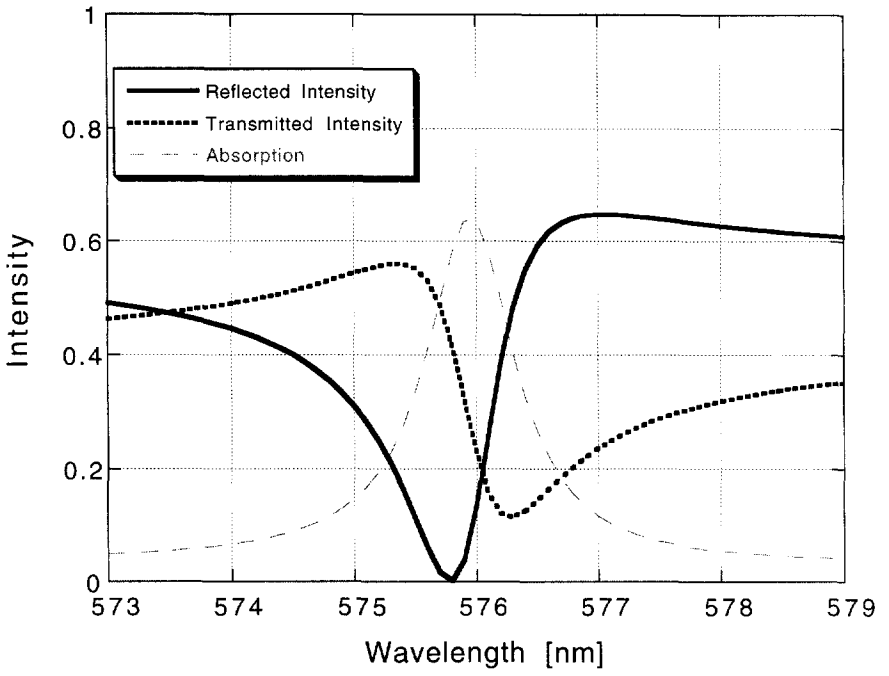

Fig. 5. Numerical calculation for the reflected and transmitted intensities and the absorption as a function of wavelength for the MB GWS which supports the long-range surface plasmon.

grating with a period of 416 nm, a height of 65 nm and a dielectric constant of 2.53, a cladding layer with thickness of 60 nm and a dielectric constant of 3.54, a silver metal layer with thickness of 20 nm and a complex dielectric constant of $-14.9+0.4i$ [24], and a substrate with dielectric constant of 2.13. Here, the thickness of the cladding layer was chosen as to produce symmetric interfaces from both sides of the metal layer. Fig. 5 shows the normalized reflected and transmitted intensities and absorption at resonance, as a function of wavelength, when the angle of the incident plane wave is oriented at 5.7 degrees with respect to the normal. The mode propagation constant, β_r, calculated from the thin grating equation, $2\pi/\Lambda = n_1 k_0 \sin\theta_i + \beta_r$, equals $1.494k_0$, in agreement with the value expected from the dispersion calculations for the multilayer model which yielded a value of $1.487k_0$. The ratio of spectral shifts between the reflection and transmission minima and the resonant wavelength is $\Delta\lambda_r/\Delta\lambda_t \cong -4/7$, versus $t_0^2/r_0^2 \cong 4/6$. A drop of the reflected intensity to zero and strong absorption of the incident plane wave are observed as well. Here, the spectral bandwidth of the reflected intensity at FWHM is about 1.2 nm.

As evident, for both cases of dielectric and metal based GWS, the ratio of the resonant shifts predicted by the analytical calculations of Section 3, is comparable with the numerical calculations. This ratio depends only on the structure reflectivity away from resonance. The calculation of the resonance line-shapes in Section 3, involved approximate values of the resonant parameters (diffraction parameter S, and the mode loss α), resulting in slight discrepancies with the numerically calculated line-shapes, where the numerical results are more exact.

5. Experimental and results

Several dielectric and metal based GWS were evaluated experimentally. The structures were formed on quartz substrates polished to a flatness of 1/10 wavelength. For the MB GWS, a silver metal layer of 20 nm thickness was formed by vapour deposition with the quartz substrate put on a surface cooled to a temperature of -196°C. This deposition technique reduced the surface roughness of the metal films as compared to films deposited at substrate temperature of 20°C [14]. The reduction of the surface roughness results in a reduction of undesirable scattering loss from the metal–cladding interface. For both, dielectric and metal based GWS, a silicon nitride layer was then formed by plasma deposition. The shallow gratings were formed by using an electron beam writing process in AZPN114 negative resist. The resist absorption at the visible region of light is negligible.

The experimental set-up for measuring and evaluating the spectral bandwidth of GWS included an argon laser for pumping a ring dye laser, and a rotating stage, whose angular orientation was accurately controlled. The beam from the dye laser was expanded and collimated to obtain a plane wave. This plane wave was incident onto the structure sample which was placed on the rotating stage. The reflected and transmitted light were collected by lenses

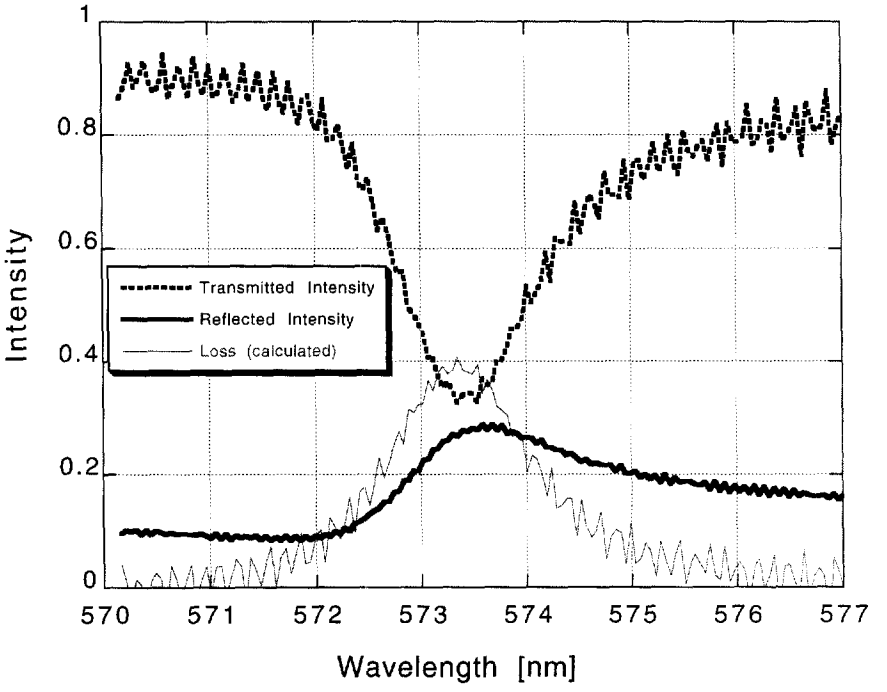

Fig. 6. Experimental results for the reflected and transmitted intensities as a function of wavelength for the dielectric GWS. Also depicted is the loss calculated as $1 - R - T$.

onto detectors. For normalization, the incident plane wave was also monitored by an additional detector. A computer was used for controlling the wavelength of the dye laser and the orientation of the rotating stage, and for monitoring all measurements from the various detectors.

Using this experimental set-up, we measured the trans-

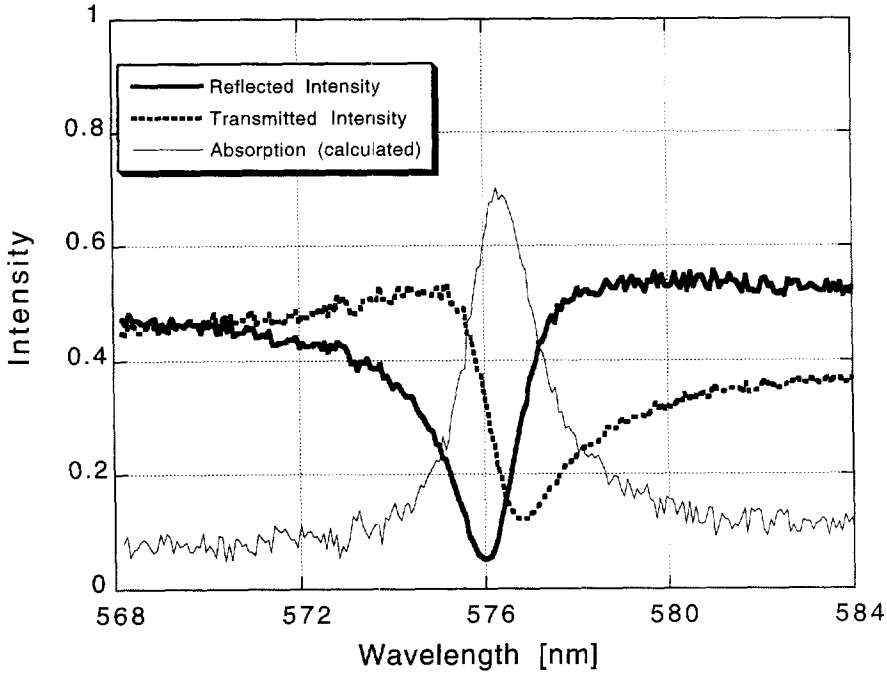

Fig. 7. Experimental results for the reflected and transmitted intensities as a function of wavelength for the MB GWS which supports the long-range surface plasmon. Also depicted is the absorption calculated as $1 - R - T$.

mitted and reflected spectral response. A representative result for a dielectric GWS, with parameters similar to the GWS of Fig. 4, is presented in Fig. 6. It shows the normalized reflected and transmitted intensities at and near resonance as a function of wavelength, when the angle of the incident plane wave is oriented at zero degrees with respect to the normal. The spectral bandwidth of the transmitted intensity at FWHM is about 1.7 nm, indicating that $\alpha \cong S$, as was assumed in the analytical and numerical calculations (see Figs. 2 and 4). The ratio of spectral shifts between the reflection and transmission minima and the resonant wavelength cannot be determined exactly, but is about $|\Delta\lambda_r/\Delta\lambda_t| \geq 9$, versus $t_0^2/r_0^2 \cong 9$. Away from resonance, $r_0^2 \cong 0.1$, $t_0^2 \cong 0.9$.

Fig. 7 shows the normalized reflected and transmitted intensities at and near resonance for a MB GWS, with parameters similar to the GWS of Fig. 5, as a function of wavelength, when the angle of the incident plane wave is oriented at 5.7 degrees with respect to the normal. With this structure, the grating couples the incident light to the long-range surface plasmon mode, for which the mode propagation constant β_r is $1.472k_0$. As shown, the minimum of the reflected intensity reaches almost zero, and the incident plane wave is strongly absorbed. The ratio of spectral shifts between the reflection and transmission minima and the resonant wavelength is $\Delta\lambda_r/\Delta\lambda_t \cong -3/4$, versus $t_0^2/r_0^2 \cong 4/5$. Here, away from resonance, $r_0^2 \cong 0.5$, $t_0^2 \cong 0.4$, and the spectral bandwidth of the reflected intensity at FWHM is about 2 nm.

As it is evident, in both cases of dielectric and metal based GWS, the resonant responses, predicted by our analytical and numerical calculations, are comparable to those observed in the experiments. The discrepancies between measured and predicted spectral, are attributed to errors in the measured structure parameters values, and to undesirable losses due to structure imperfections.

6. Concluding remarks

We investigated, both theoretically and experimentally, the resonant response of GWS, with sufficient generality to account for asymmetry of the response. Specifically, we identified an interference effect which is responsible for the asymmetries of the resonance line-shapes. We found a simple rule that allowed us to quantify these resonant asymmetries, using the off-resonance properties of the GWS. The theoretical predictions were verified experimentally with dielectric and metal based GWS. These investigations point to the various tradeoffs that should be taken into account when designing GWS for specific applications. In general, the resonant responses are asymmetric, but these responses become symmetric in the limiting cases where the GWS are either fully reflective or completely transparent away from resonance.

Acknowledgements

We thank Maya Sharon for her assistance with the computer simulations, and the partial support from the Israel Ministry of Science and Arts.

References

[1] R.W. Wood, Phil. Mag. 4 (1902) 396.
[2] Lord Rayleigh, Proc. R. Soc. A 79 (1907) 399.
[3] U. Fano, J. Opt. Soc. Am. 31 (1941) 213.
[4] R.H. Ritchie, Phys. Rev. 106 (1957) 874.
[5] A. Hessel, A.A. Oliner, Appl. Optics 4 (1965) 1275.
[6] M. Neviere, in: R. Petit (Ed.), Electromagnetic Theory of Gratings, Springer, Berlin, 1980, Ch. 5.
[7] G.A. Golubenko, A.S. Svakhin, V.A. Sychugov, A.V. Tishchenko, Sov. J. Quantum Electron. 15 (1985) 886.
[8] E. Popov, L. Mashev, D. Maystre, Optica Acta 33 (1986) 607.
[9] I.A. Avrutskii, V.A. Sychugov, Sov. Phys. Tech. Phys. 32 (1987) 235.
[10] S.S. Wang, R. Magnusson, J.S. Bagby, M.G. Moharam, J. Opt. Soc. Am. A 7 (1990) 1470.
[11] A. Sharon, D. Rosenblatt, A.A. Friesem, H.G. Weber, H. Engel, R. Steingrueber, Optics Lett. 21 (1996) 1564.
[12] M.T. Gale, K. Knop, R.H. Morf, Proc. SPIE Optic. Security Anticounterfeiting Syst. 1210 (1990) 83.
[13] A. Sharon, D. Rosenblatt, A.A. Friesem, Appl. Phys. Lett. 69 (1997) 4154.
[14] S. Glasberg, A. Sharon, D. Rosenblatt, A.A. Friesem, Appl. Phys. Lett. 70 (1997) 1210.
[15] K. Berthold, W. Beinstingl, E. Gornik, Optics Lett. 12 (1987) 69.
[16] A. Sharon, S. Glasberg, D. Rosenblatt, A.A. Friesem, J. Opt. Soc. Am. A 14 (3) (1997) 588.
[17] R.W. Day, S.S. Wang, R. Magnusson, J. Lightwave Technol. 14 (1996) 1815.
[18] A. Hardy, D.F. Welch, W. Streifer, in: G.A. Evans, J.M. Hammer (Eds.), Surface Emitting Semiconductor Lasers and Arrays, Academic Press, New York, 1993, Ch. 6.
[19] H. Raether, Surface plasmons on smooth and rough surfaces and on gratings, Springer, New York, 1988.
[20] A. Yariv, Optical Electronics, 3rd ed., Holt, Rhinehart & Winston, 1985.
[21] D. Sarid, Phys. Rev. Lett. 47 (1981) 1927.
[22] J.J. Burke, G.I. Stegeman, T. Tamir, Phys. Rev. B 33 (1986) 5186.
[23] P. Sheng, R.S. Steplman, P.N. Sanda, Phys. Rev. B 26 (1982) 2907.
[24] P.B. Johnson, R.W. Christy, Phys. Rev. B 6 (1972) 4370.